Analytical and Numerical Approaches for the Computation of Aeroelastic Sensitivities Using the Direct and Adjoint Methods

Lukas Scheucher

Stanford University

October 2016 - June 2017

Overview

Outline for section 1

The compressible Navier Stokes equations in conservative form can be written as

$$\underbrace{\frac{\partial \bar{\boldsymbol{w}}}{\partial t}}_{\text{time derivative}} + \underbrace{\nabla \cdot \mathcal{F}(\bar{\boldsymbol{w}})}_{\text{inviscid}} + \underbrace{\nabla \cdot \mathcal{G}(\bar{\boldsymbol{w}})}_{\text{viscous}} = \underbrace{\mathsf{S}(\bar{\boldsymbol{w}}, \chi_1, \cdots, \chi_m)}_{\text{source term}}$$

Inviscid fluxes

$$\mathcal{F} = \boldsymbol{w}\boldsymbol{v}^T + p \begin{bmatrix} 0 \\ \mathsf{I} \\ \boldsymbol{v}^T \end{bmatrix}$$

Viscous fluxes

$$\mathcal{G} = \begin{bmatrix} \mathbf{0} \\ \boldsymbol{\tau} \\ \boldsymbol{\tau}\boldsymbol{v} + \boldsymbol{q} \end{bmatrix}$$

Mesh is structure specific

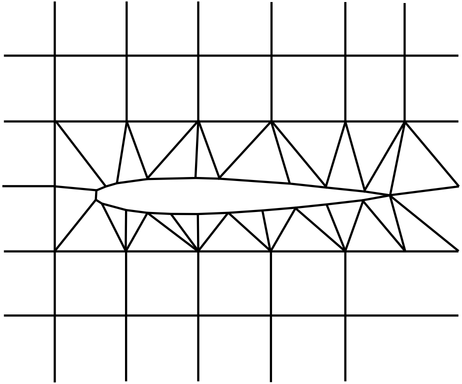

Figure: Body-fitted

Mesh is structure specific

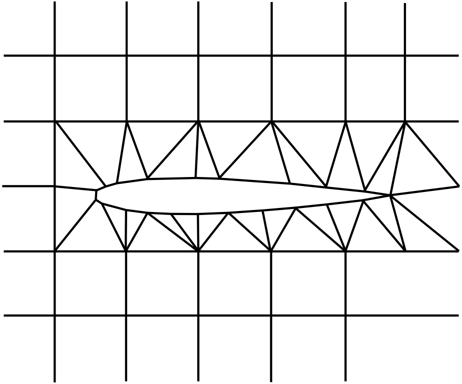

Figure: Body-fitted

Mesh independent of structure geometry

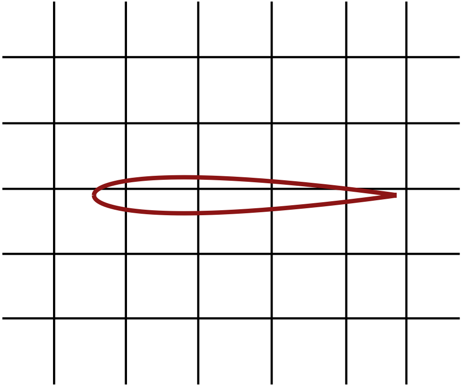

Figure: Embedded

Immersed Boundary Method
FIVER[1]

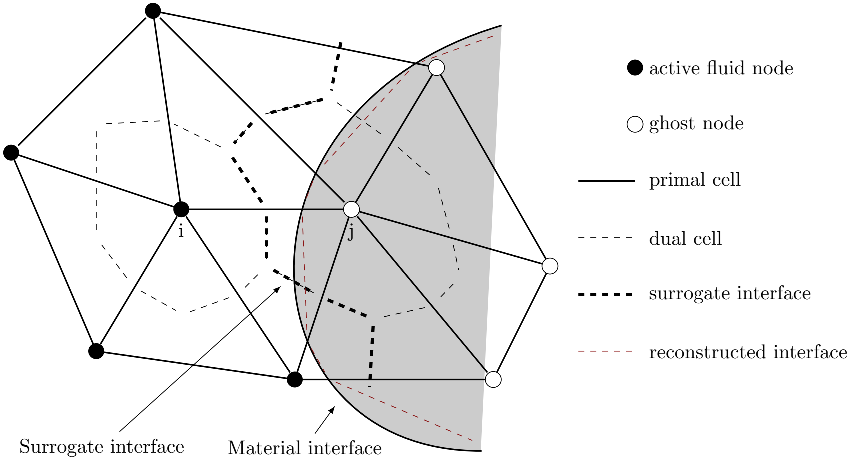

[1]**Main2014**.

- Body-fitted and Immersed boundaries (FIVER)
- FE-like treatment of the visocus term

$$\frac{\partial \boldsymbol{w}_i}{\partial t} + \int_{\partial \mathcal{C}_i} \mathcal{F}(\boldsymbol{w}) \cdot dS - \int_{\sum_{T_i}} \mathbb{K}\boldsymbol{w}\nabla\phi_i dx = \mathbf{0}$$

$$\int_{\partial \mathcal{C}_i} \mathcal{F}(\boldsymbol{w}) \cdot dS \approx \underbrace{\sum_{j \in \kappa(i)^a} \boldsymbol{\phi}_{ij}(\boldsymbol{w}_i, \boldsymbol{w}_j, \boldsymbol{\nu}_{ij})}_{\text{non-intersected elements}} + \underbrace{\sum_{j \in \kappa(i) \setminus \kappa(i)^a} \boldsymbol{\phi}_{ij}(\boldsymbol{w}_i, \boldsymbol{w}^*, \boldsymbol{\nu}_{ij})}_{\text{intersected elements treated with FIVER}}$$

ϕ ... flux function of Roe[2]

[2]**Roe1981**.

- Identify immersed boundaries with control volume interfaces $\mathcal{C}_{ij}$

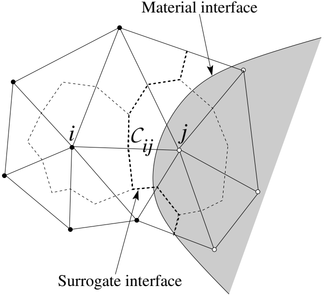

- Solve exactly local one-dimensional half-Riemann problems at $\mathcal{C}_{ij}$

$$\begin{cases} \dfrac{\partial \tilde{\mathbf{w}}^\star}{\partial \tau} + \dfrac{\partial \tilde{\mathbf{f}}(\tilde{\mathbf{w}}^\star)}{\partial \xi} = 0 \\ \tilde{\mathbf{w}}^\star(\xi, 0) = \tilde{\mathbf{w}}_{ij}, & \xi \leq 0 \\ \boldsymbol{v}(0,\tau) \cdot \mathbf{n}_{\text{wall}} = \boldsymbol{v}_{\text{wall}} \cdot \mathbf{n}_{\text{wall}}, & 0 \leq \tau \leq \Delta t \end{cases}$$

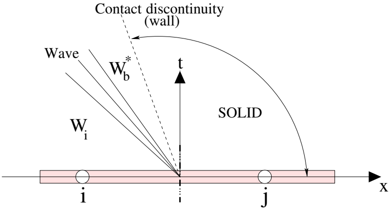

- Evaluate numerical flux: $\mathbf{F}_{ij} = \mathbf{F}_{ij}(\mathbf{w}_{ij}, \mathbf{w}_b^\star, \boldsymbol{n}_{ij})$

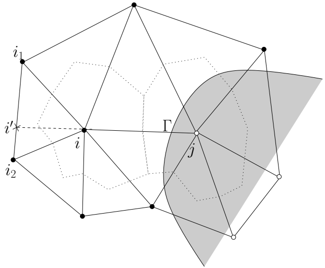

- The fluid state is extrapolated to the material interface Γ
$$\mathbf{w}_\Gamma = \mathbf{w}_i + \nabla \mathbf{w}_i \cdot (\mathbf{x}_\Gamma - \mathbf{x}_i)$$
- The one-dimensional half-Riemann problem is solved at material interface Γ
$$\tilde{\mathbf{w}}_\Gamma^\star = \tilde{\mathbf{w}}^\star(\tilde{\mathbf{w}}_\Gamma, \boldsymbol{v}_{\text{wall}}, \mathbf{n}_{\text{wall}})$$
- The fluid state is inter/extra-polated at control volume interface $\mathcal{C}_{ij}$
$$\mathbf{w}_{ij}^\star = \mathbf{w}_{ij}^\star(\mathbf{w}_\Gamma^\star, \mathbf{w}_{i'})$$
- Numerical flux at the control volume interface: $\mathbf{F}_{ij} = \mathbf{F}_{ij}(\mathbf{w}_{ij}, \mathbf{w}_{ij}^\star, \boldsymbol{n}_{ij})$
- Second-order convergence is recovered in the vicinity of the interface

Outline for section 2

Multi-element airfoil with large kinematics
Prime example for embedded framework

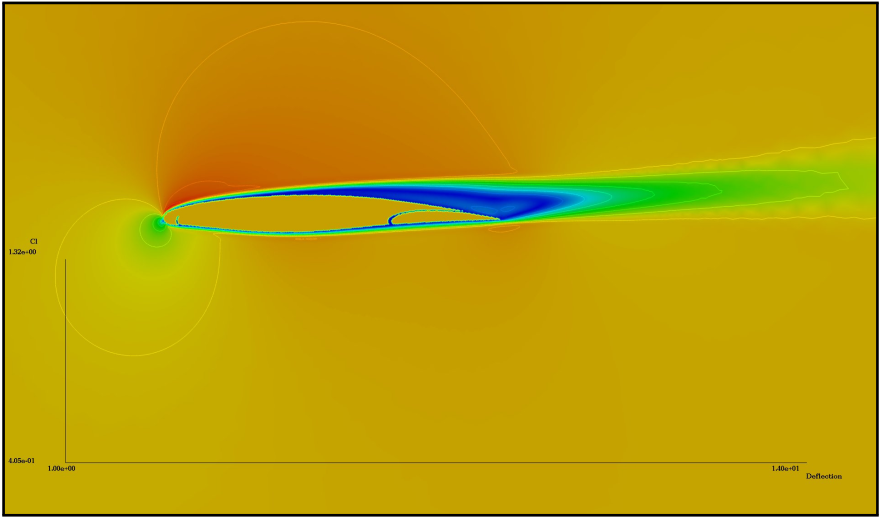

Figure: Optimization iteration 1

Multi-element airfoil with large kinematics
Prime example for embedded framework

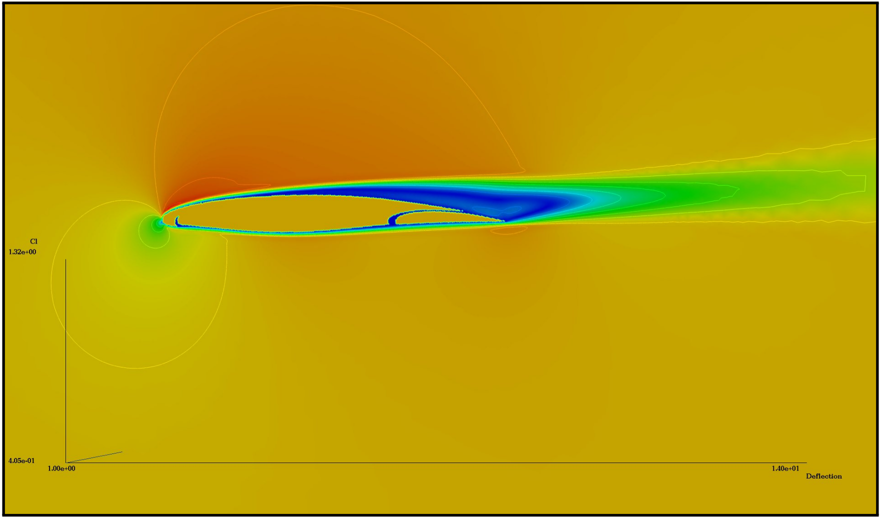

Figure: Optimization iteration 2

Multi-element airfoil with large kinematics
Prime example for embedded framework

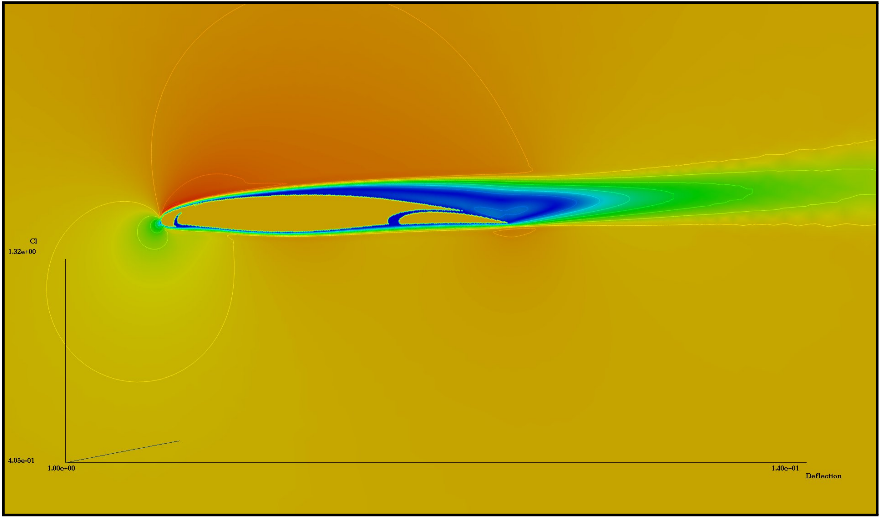

Figure: Optimization iteration 3

Multi-element airfoil with large kinematics
Prime example for embedded framework

Multi-element airfoil with large kinematics
Prime example for embedded framework

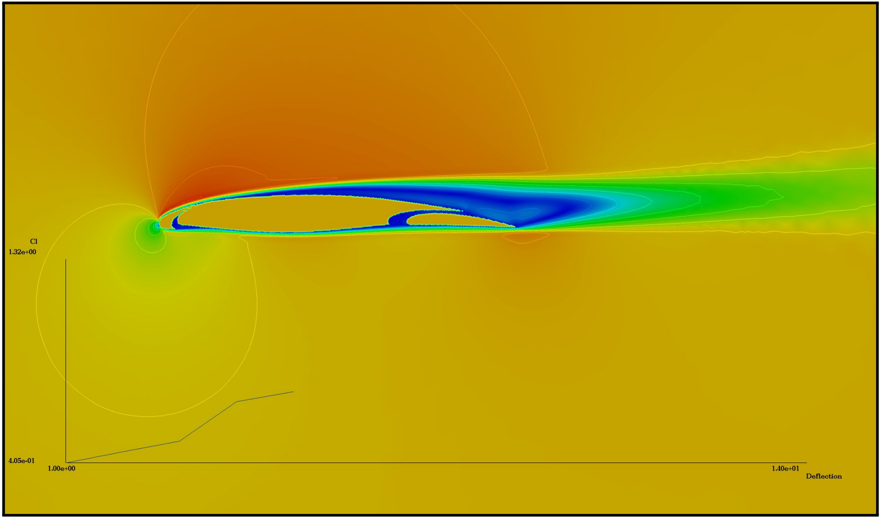

Figure: Optimization iteration 5

Multi-element airfoil with large kinematics
Prime example for embedded framework

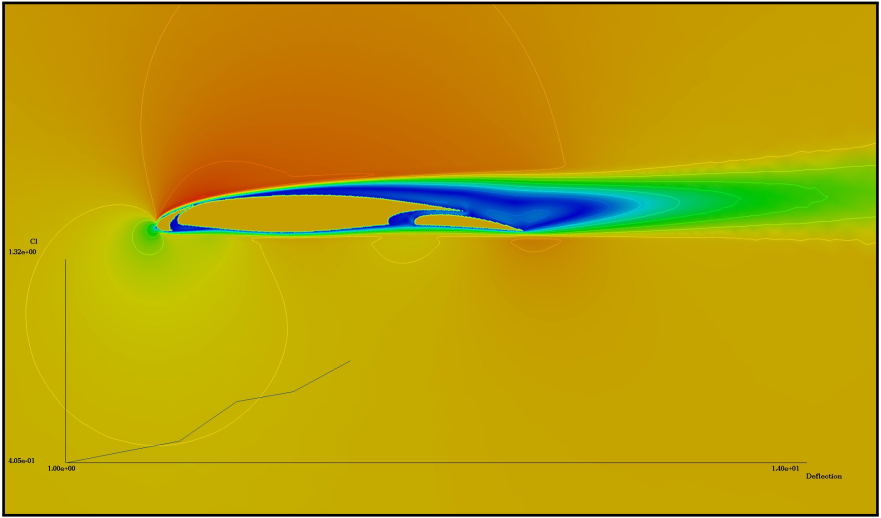

Figure: Optimization iteration 6

Multi-element airfoil with large kinematics
Prime example for embedded framework

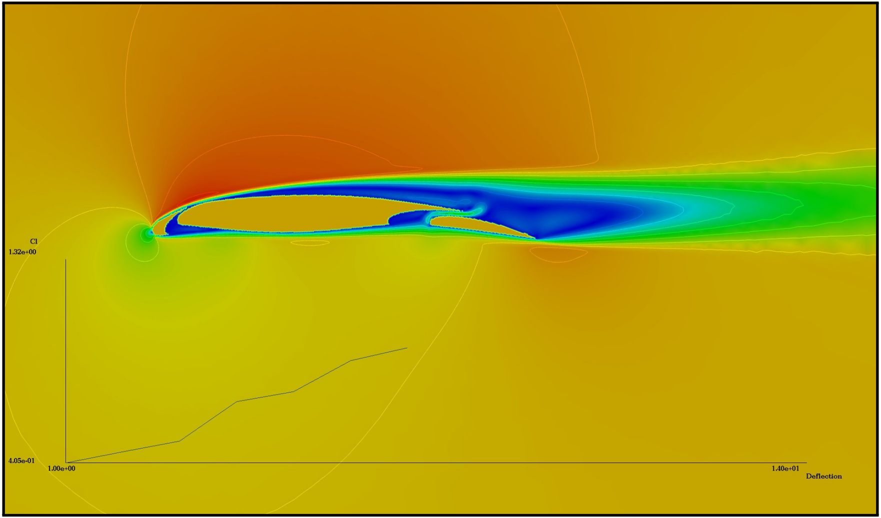

Figure: Optimization iteration 7

Multi-element airfoil with large kinematics
Prime example for embedded framework

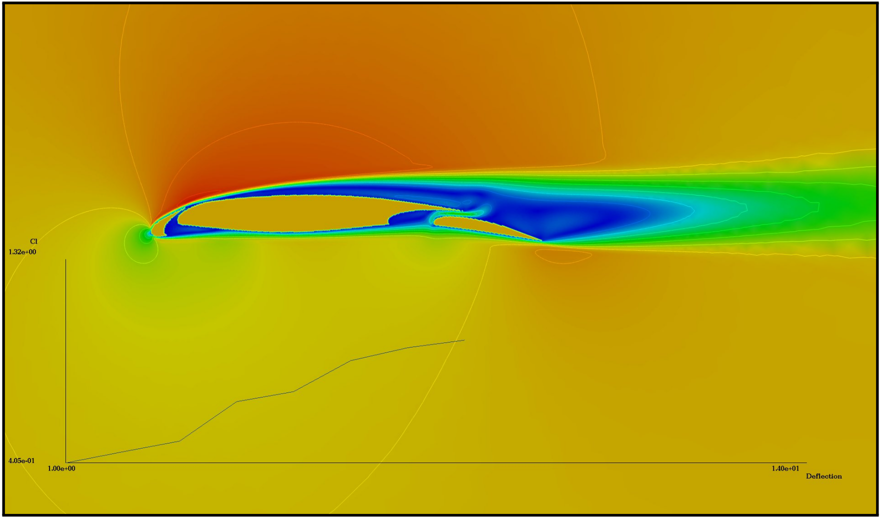

Figure: Optimization iteration 8

Multi-element airfoil with large kinematics
Prime example for embedded framework

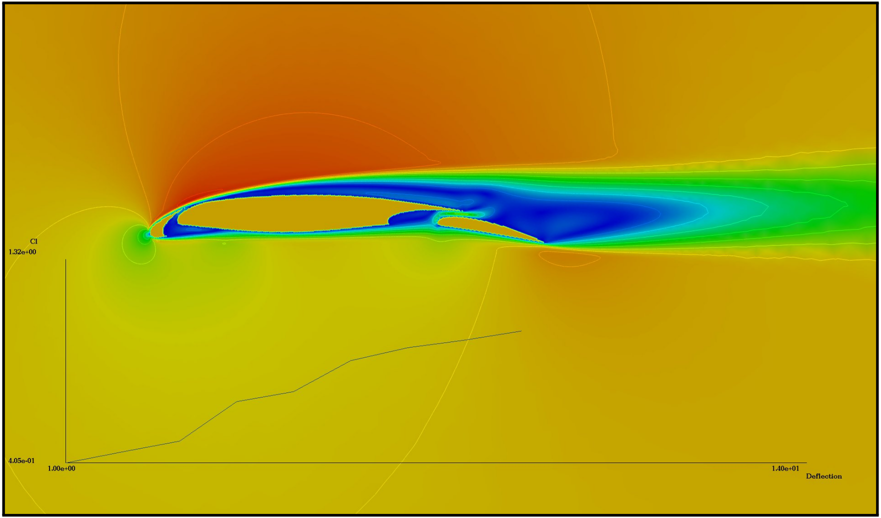

Figure: Optimization iteration 9

Multi-element airfoil with large kinematics
Prime example for embedded framework

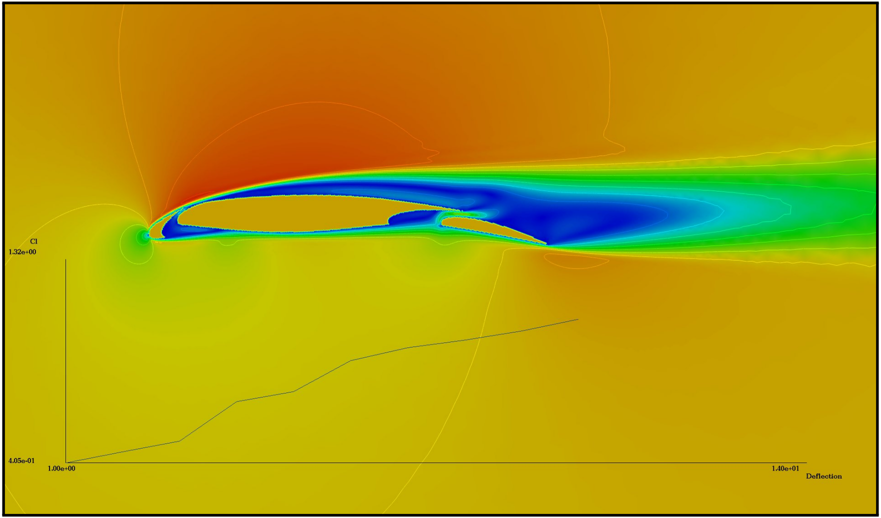

Figure: Optimization iteration 10

Multi-element airfoil with large kinematics
Prime example for embedded framework

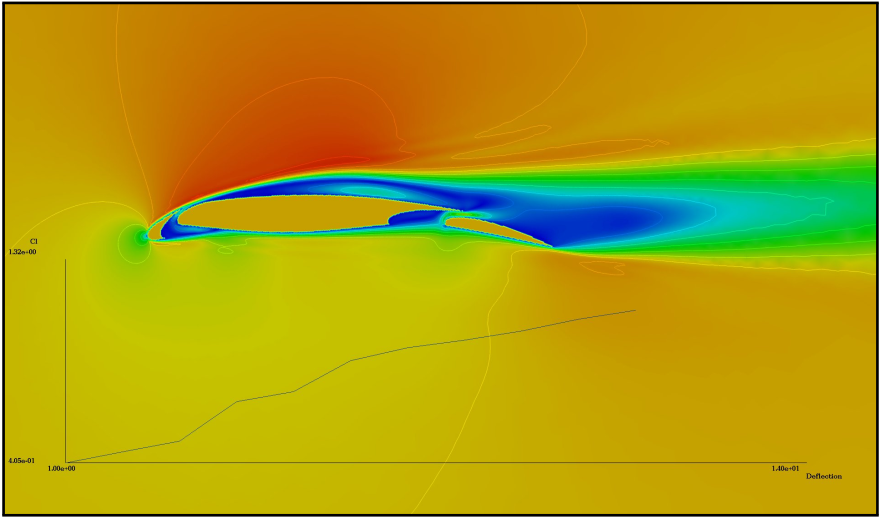

Figure: Optimization iteration 11

Multi-element airfoil with large kinematics
Prime example for embedded framework

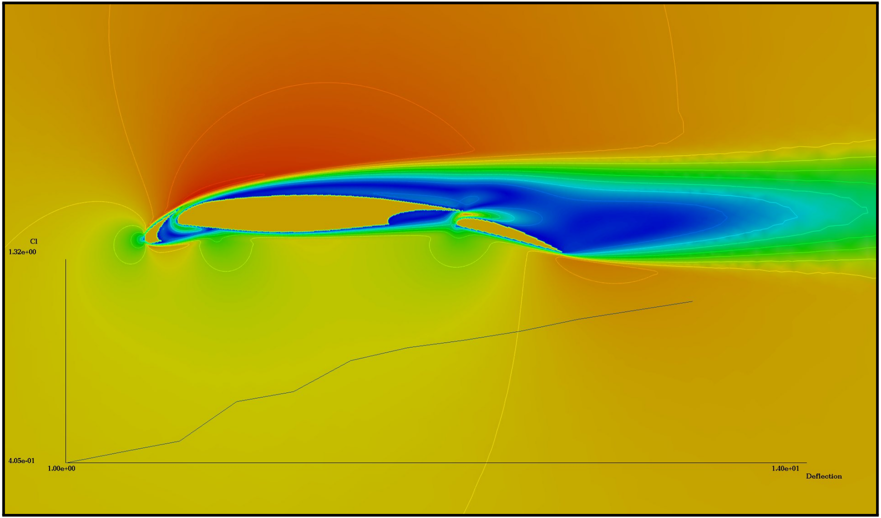

Figure: Optimization iteration 12

Multi-element airfoil with large kinematics

Prime example for embedded framework

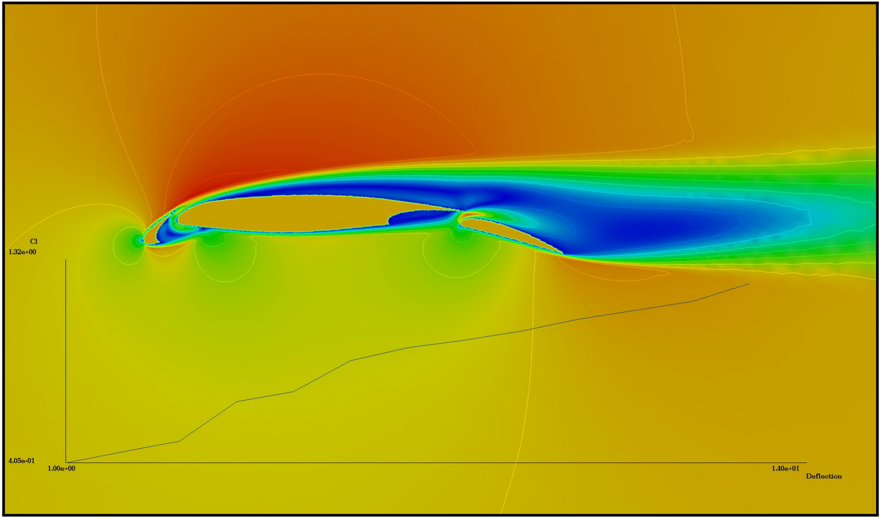

Figure: Optimization iteration 13

Multi-element airfoil with large kinematics
Prime example for embedded framework

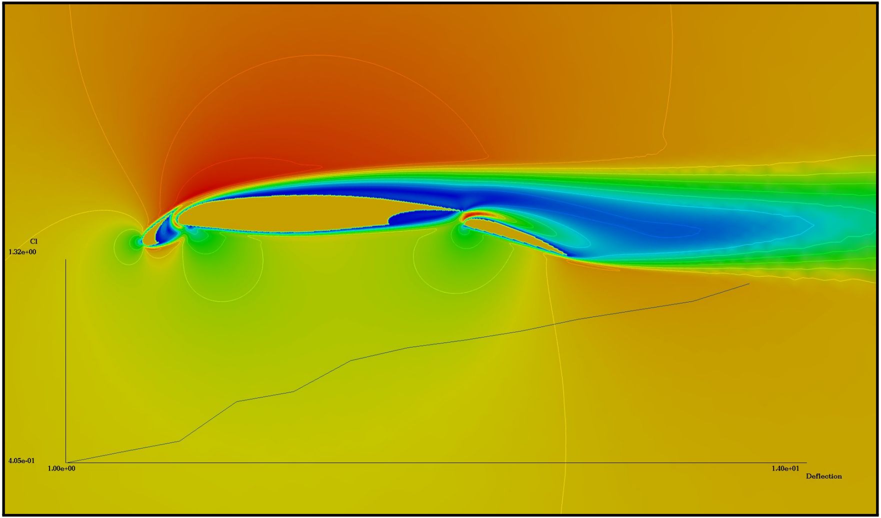

Figure: Optimization iteration 14

Multi-element airfoil with large kinematics
Prime example for embedded framework

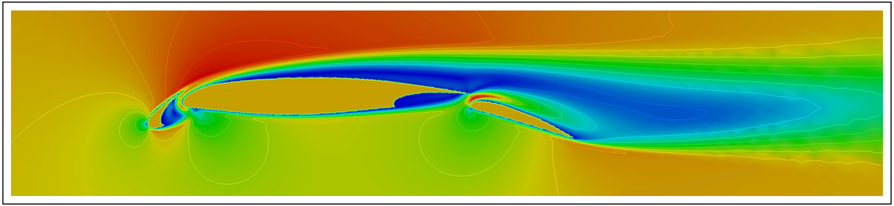

- $M = 0.2$ and $\alpha = 10°$
- Starting from closed configuration; let optimizer find the best relative positions of the airfoil elements
- 6 design variables: rotation, vertical and horizontal displacement of the elements
- Final value of the lift doubles after 6 optimization iterations